phys. stat. sol. (c) **2**, No. 7, 2441 – 2445 (2005) / **DOI** 10.1002/pssc.200461482

Comparison of GaMnN epilayers prepared by ion implantation and metalorganic chemical vapor deposition

M. H. Kane[*,1,2], **A. Asghar**[2], **A. M. Payne**[2], **C. R. Vestal**[3], **Z. J. Zhang**[3], **M. Strassburg**[2,4], **J. Senawirante**[4], **N. Dietz**[4], **C. J. Summers**[1], and **I. T. Ferguson**[2]

[1] School of Materials Science and Engineering, Georgia Institute of Technology, Atlanta, GA 30332-0245, USA
[2] School of Electrical and Computer Engineering, Georgia Institute of Technology, Atlanta, GA 30332-0250, USA
[3] School of Chemistry and Biochemistry, Georgia Institute of Technology, Atlanta, GA 30332-0400, USA
[4] Department of Physics and Astronomy, Georgia State University, Atlanta, GA 30303-4106, USA

Received 12 July 2004, revised 17 September 2004, accepted 24 January 2005
Published online 17 March 2005

PACS 61.72.Vv, 75.50.Pp, 75.70.Ak, 78.55.Cr, 81.05.Ea, 81.15.Gh

The ferromagnetic semiconductor GaMnN has been produced by two methods – ion implantation and metalorganic chemical vapor deposition (MOCVD). P-type, n-type, and intrinsic GaN layers grown by MOCVD were ion-implanted with 3 x 10^{16}/cm^2 Mn^+ at 200 keV and subsequently annealed under various conditions. Considerable lattice damage is observed by analyzing the peak asymmetry in X-ray diffraction; annealing only partially recovers this damage. Second phases (Mn_xN_y, Ga_xMn_y and $Mn_{4-x}Ga_xN_{1-y}$) have been detected upon subsequent annealing. Epitaxial GaMnN layers have been fabricated by MOCVD using Cp_2Mn as the manganese precursor. These films were specular and exhibited an increasing dark reddish-brown tinge with increasing Mn-concentration and thickness, consistent with GaMnN grown by other methods. X-ray diffraction revealed symmetric peaks with almost identical lattice parameters to undoped GaN, and no macroscopic second phase formation. Magnetic hysteresis is observed in the ion implanted as well as in MOCVD-grown films at room temperature. Stronger magnetization was present in the implanted p-type films and unannealed MOCVD-grown films, providing evidence that Fermi level control is important for the magnetic properties of these materials.

1 Introduction

Nitride-materials have been the subject of considerable interest over the past few years for applications in the field of spintronics. Theoretical predictions [1] have indicated that when alloyed with small percentages of transition-metal elements, GaN can exhibit ferromagnetic behavior at temperatures much greater than the cryogenic levels of traditional dilute magnetic semiconductors (DMS). There are several experimental reports of GaMnN which exhibit ferromagnetism above room temperature [2–4]. Still, it is not well understood whether the ferromagnetism derives from an intrinsic material property or from nanoscaled cluster distributions in the system. Until a method for optimizing the structure-property-processing characteristics of these materials exists, future room-temperature spintronic applications will be difficult.

* Corresponding author: e-mail: mhkane@ece.gatech.edu

It is imperative to note that the well-accepted arsenide DMS are grown by techniques such as low-temperature molecular beam epitaxy (LT-MBE) in order to avoid phase segregation. As this technique uses a non-equilibrium growth method at a temperature that minimizes diffusion during growth, it can be termed far-from-equilibrium. On the other hand, the nitride materials have not necessarily been produced by such far-from-equilibrium techniques, using techniques which require either elevated temperature or post-growth elevated temperature processing. This work compares two techniques for fabrication of GaMnN: ion implantation and MOCVD. Ion implantation is useful for introducing transition metal atom concentrations well above the equilibrium solubility limit and almost universally results in room temperature ferromagnetic behavior in Mn-doped semiconductors [5], even in GaAs:Mn [6]. This technique, however, results in an inhomogeneous distribution of the TM ions, and thus is not ideal for spintronic integrated devices. MOCVD may be able to overcome these problems, since it is the technique of choice for optical quality device structures in this materials system. It should be noted, that InMnAs layers grown by MOCVD exhibits vastly different behavior compared to LT-MBE InMnAs, with nominally phase-pure MOCVD grown material exhibiting a Curie temperature of 330 K [7]. Whether MOCVD grown GaMnN will exhibit a similar clustering tendency as in InMnAs has to be determined.

2 Experimental procedure

MOCVD grown layers, p-type ($p = 2 \times 10^{16}/cm^3$), n-type ($n = 6 \times 10^{17}/cm^3$), and intrinsic GaN were ion-implanted with Mn concentrations of $3 \times 10^{16}/cm^2$ at an energy of 200 keV and a substrate temperature of 400 °C. In order to remove the implantation damage, samples were subsequently annealed face-down on GaN templates in a flowing nitrogen ambient at temperatures ranging from 700 °C to 900 °C. GaMnN films with Mn concentration up to ~2% were also grown at standard GaN growth temperatures. Initially, two micron thick GaN buffer layer templates were grown using standard GaN techniques on c-sapphire. Ammonia, trimethyl gallium (TMG) and bis-cyclopentadienyl manganese (Cp_2Mn), bis-cyclopentadienyl magnesium (Cp_2Mg) and silane (SiH_4) were used as the nitrogen, gallium, manganese, p-, and n-dopant sources respectively for the GaMnN. Subsequent characterization of these films was performed, including X-ray diffraction (XRD), secondary ion mass spectroscopy (SIMS), and superconducting quantum interference device magnetometry (SQUID).

3 Results and discussion

XRD $2\theta-\omega$ scans for the ion implanted samples before and after annealing are shown in Figure 1, along with the scan for an undoped GaN layer on c-sapphire. The scans are similar for the undoped and as implanted sample, with the exception of a distinct elbow and tail on the low angle side of the peak due to the large local Mn concentration and predominantly interstitial defects in the implanted samples. After annealing, this low-angle peak shelf is still visible indicating the damage is not fully recovered. In addition, in some of the annealed samples, additional XRD peaks are observed. The peak at 32.4 ° most closely to either the metallic perovskite phase $Mn_{4-x}Ga_xN_{1-y}$ or the intermetallic Mn_8Ga_5. Also visible in some scans are peaks from the antiferromagnetic compounds $Mn_6N_{2.58}$ and Mn_3N_2. Similar non-stoichiometric phases have been observed previously in MBE grown [8] and heavily-annealed implanted samples [9]. Ion implantation introduces an excess of Gallium site cations; the annealing conditions are not suitable for the replenishment of nitrogen and subsequent rearrangement of a 1:1 stoichiometric crystalPhase separation can occur even at temperatures that have been reported as suitable for GaMnN annealing [9].

The reddish colored MOCVD-grown layers show a uniform Mn depth profile as analyzed by SIMS. This suggests a homogeneous incorporation of the Mn up to a few percent (<3%) in the lattice. X-ray diffraction scans on the MOCVD-grown GaMnN samples are depicted in Fig. 1. The peak position and shape are very similar to that for the undoped GaN sample. No statistically significant deviation in the lattice parameter was observed, even for Mn concentrations in the order of ~2% (as estimated from the

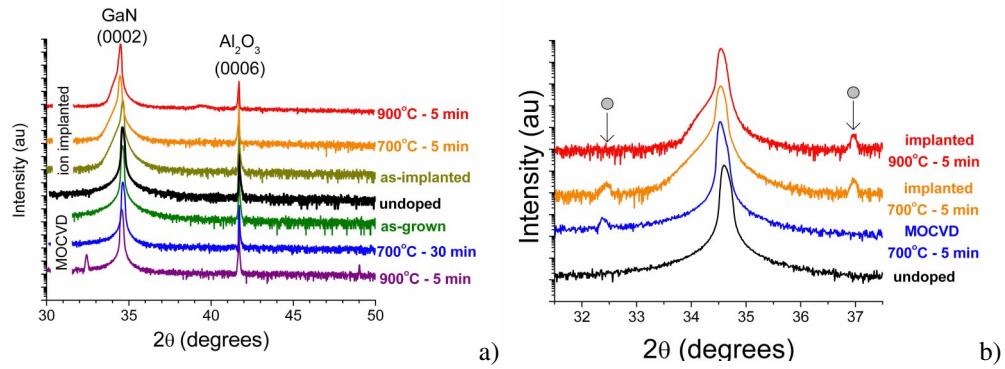

Fig. 1 a) XRD scans for undoped GaN, implanted, and MOCVD-grown GaMnN before and after annealing. Note the shoulder on all the implanted GaN (0002) peaks, as well as the appearance of additional phases w/high temperature annealing. b) Close-up of different scans on implanted and MOCVD grown GaMnN, showing the appearance of Mn_xN_y, Ga_xMn_y, and/or $Mn_{4-x}Ga_xN_{1-y}$ phases at annealing temperatures as low as 700 °C.

growth conditions). There is also little change in the 2θ–ω scan linewidths (179, 196, and 251 arcsec for the undoped, 0.3%, and 2.25% Mn 2θ–ω scans, respectively) or rocking curve widths of the symmetric and asymmetric reflections. In contrast to the Mn-ion implanted samples, the GaN (0002) peak is symmetric, indicating little macroscopic strain with Mn incorporation. There are indications of the presence of the forbidden (0001) and (0003) peaks in the doped Mn-layers, which have been previously observed in diffusion-grown GaMnN [2]. These additional reflections are only seen in the Mn-doped samples and may be due to local structural imperfections due to compensation effects from the heavy Mn doping.

Squid magnetometry was used to examine implanted and annealed as well as MOCVD-grown samples. The magnetization vs. field results are shown for an implanted intrinsic, p-type, and n-type GaN sample in Fig. 2a. In this diagram, it is clear that for both the n-type and nominally intrinsic sample, clear hysteresis is visible in the curves at room temperature. The Curie temperature in both cases is well above RT, as observed by M vs. H curves. All of the implanted samples are of roughly the same size, but the SQUID signal from the p-type GaMnN must be multiplied by a factor of one tenth to fit on the same scale as the other two samples. All three samples (p-type, intrinsic, and n-type) show clear hysteresis

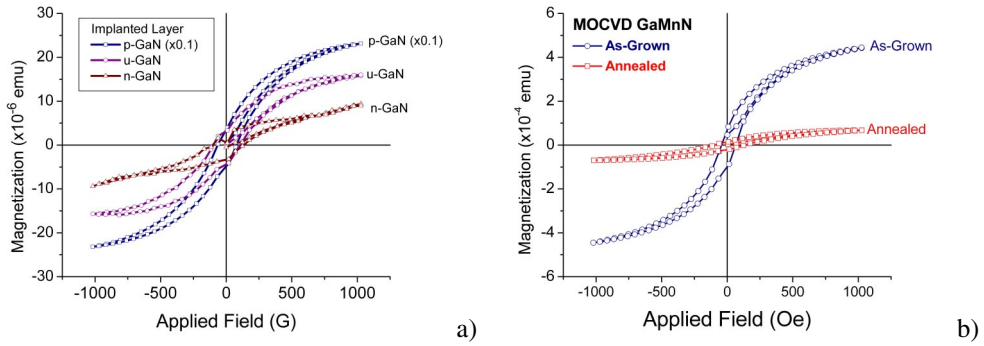

Fig. 2 M vs. H curves for a) implanted and annealed p-type, n-type, and intrinsic GaN taken at 300 K. The p-type curve has been divided by a factor of 10. b) As-grown MOCVD $Ga_{1-x}Mn_xN$ (x = 0.008) taken at 300 K, and 800 °C-annealed MOCVD $Ga_{1-x}Mn_xN$ (x = 0.008) measured at (5K), with ferromagnetic-like magnetic behavior in both samples. The magnetization decreases considerably with annealing.

with coercivities of around 50 Oe and saturation to remnant magnetization ratios of 0.1–0.2. The source of this ferromagnetism in the intrinsic and n-type samples may still be due to the macroscopic alloy, unobserved second phases, or Mn-rich clusters in the as-grown system The magnetic signal decreases as doping goes from p- to n-, with the largest signal observed in the p-type sample. Figure 2b shows the M vs. H curves for an MOCVD-grown film both before annealing Though the deep nature of the Mn acceptor in GaN [10] results in carrier concentrations lower than required by the mean-field mode for RT ferromagnetism, the as-grown GaMnN layers, the films still exhibit room temperature magnetic hysteresis at concentrations of ~0.8% Mn, as shown in Fig. 2b. Significant changes are observed in the magnetic behavior due to annealing of the layers. From an estimate of the film volume, there is a relatively large (~3 μ_B/Mn) magnetic contribution per magnetic dopant to the saturization magnetization prior to annealing, as observed in lightly-doped diffusion grown GaMnN [11].

The reasons for the drastic difference in the magnetic behavior in these samples may be understood as a function of the valence state of the Mn ion. For both the mean field and double exchange mechanisms to be valid, Mn must be in the 3+ valence state [12], either as d^4 or d^5 + hole; Mn^{2+} is GaN is expected and observed to lead to paramagnetism. Several mechanisms could lead to the decrease is ferromagnetism in these samples with annealing. Increased antiferromagnetic Mn-Mn superexchange interactions would result from Mn atom nearest-neighbor clustering. In addition, secondary phases, including the antiferromagneic Mn_xN_y compounds are known to form at elevated temperatures annealing [9].Annealing in a nitrogen atmosphere also drives out any residual hydrogen from the layers; hydrogen has been shown to aid the magnetic behavior by passivation of defect states [13]. Similarly, annealing can introduce a nitrogen vacancies which act as shallow donors, driving the Fermi level towards the valence band. Given that the strong ferromagnetism is seen in the p-type implanted sample and the as-grown MOCVD sample, Fermi level control by keeping E_F less than the $Mn^{2+/3+}$–acceptor level leads to enhanced ferromagnetic behavior in the GaMnN dilute magnetic semiconductor system.

4 Conclusion

GaMnN exhibiting room temperature ferromagnetism has been produced by ion implantation and metalorganic chemical vapor deposition. MOCVD results in high quality material, whereas ion implantated layers retained significant damage even after annealing. Though the material is initially single phase, post growth processing results in the appearance of second phases (Mn_xN_y, $Mn_{4-x}Ga_xN_{1-y}$) in the X-ray diffraction scans. These phases can occur even under anneals at relatively low temperature in the nitride materials, indicating a need to minimize post-processing in these materials. Magnetic hysteresis was observed in all samples regardless of carrier type, indicating that under the growth conditions small amounts of second phases could possibly form under these growth conditions. The strength of the magnetization is an order of magnitude stronger in the p-type implanted material relative to the n-type material; in addition, the MOCVD-grown material exhibited an order of magnitude drop in the magnetization after a high temperature anneal. These results suggest that Fermi level control, specifically keeping E_F below the $Mn^{3+/2+}$ acceptor level, is crucial for the magnetic behavior in the GaMnN system

Acknowledgements This work was supported in part by grants from the National Science Foundation (ECS#0224266, U. Varshney) and Air Force Office of Scientific Research (T. Steiner). One author (M.K.) was supported by a National Defense Science and Engineering Graduate Fellowship sponsored by the Department of Defense. M.S. gratefully acknowledges the fellowship of the Alexander von Humboldt-Foundation. The authors thank D. Nicol for performing the annealing steps.

References

[1] T. Dietl et al.. Science. **287**, 1019–1022 (2000).
[2] M.L. Reed et al., Appl. Phys. Lett. **79**, 3473–3475 (2001).
[3] S. Sonoda et al., IEEE Trans. Magn. **38**, 2859–2862 (2002).

[4] N. Theodoropoulou et al., Appl. Phys. Lett. **78**, 3475–3477 (2001).
[5] N. Theodoropoulou et al., J. Appl. Phys. **91**, 7499–7501 (2002).
[6] J. Shi et al., J. Appl. Phys. **79**, 5296–5298 (1996).
[7] A.J. Blattner, J. Lensch, and B.W. Wessels, J. Electron. Mater. **30**, 1408–1411 (2001).
[8] G.T. Thaler et al., Electrochem. Solid State Lett. **7**, G34–G36 (2004).
[9] J.M. Baik et al., J. Appl. Phys. **93**, 9024–9029 (2003).
[10] T. Graf et al.. Appl. Phys. Lett. **81**, 5159–5161 (2002).
[11] M.L. Reed et al., Mater. Ress. Soc. Symp. Proc. **798**, Y8.6.1 (2004).
[12] T. Dietl, phys. stat. sol. (b) **240**, 433–439 (2003).
[13] K.H. Baik et al., Appl. Phys. Lett. **83**, 5458–5460 (2003).